Journal of Organometallic Chemistry 694 (2009) 3800–3805

Contents lists available at ScienceDirect

Journal of Organometallic Chemistry

journal homepage: www.elsevier.com/locate/jorganchem

Novel diazadienes based on 1,3,4-oxadiazines: Ligands in iron carbonyl complexes and substrates in catalytic [2+2+1] cycloaddition reactions

Katharina Kaleta [a], Jan Fleischhauer [b], Helmar Görls [a], Rainer Beckert [b], Wolfgang Imhof [a,*]

[a] Institute of Inorganic and Analytical Chemistry, Friedrich-Schiller-University Jena, August-Bebel-Str. 2, D-07743 Jena, Germany
[b] Institute of Organic Chemistry and Macromolecular Chemistry, Friedrich-Schiller-University Jena, Humboldtstr. 10, D-07743 Jena, Germany

ARTICLE INFO

Article history:
Received 15 May 2009
Received in revised form 6 July 2009
Accepted 10 July 2009
Available online 16 July 2009

Keywords:
Iron
Ruthenium
Carbonyl complexes
Catalysis
Cycloaddition
Lactams

ABSTRACT

N,*N*′-(4-methyl-4*H*-1,3,4-oxadiazine-5,6-diylidene)-bis-aniline derivatives react with $Fe_2(CO)_9$ to give dinuclear iron carbonyl complexes. One of the iron atoms is bonded symmetrically to both exocyclic imine nitrogen atoms. The second iron atom shows a side-on coordination towards the C=N bond next to the oxadiazine oxygen atom. In addition, the iron atoms are connected *via* a metal metal bond. The same oxadiazine derivatives produce chiral spiro-lactams in a ruthenium catalyzed formal [2+2+1] cycloaddition reaction with carbon monoxide and ethylene.

1. Introduction

Cycloaddition reactions represent one of the most atom economic and straightforward synthetic strategies for the production of carbocyclic or heterocyclic organic compounds. During the last decades a number of cycloaddition reactions catalyzed by transition metals have been reported and the progress of this field of research has been thoroughly reviewed [1]. We have been able to show that chiral diazadienes from the reaction of enantiomerically pure *S*-prolinol with *N*,*N*′-bis-aryl-oxalimidoylchlorides may be reacted either with $Fe_2(CO)_9$ under thermal or with $Fe(CO)_5$ under photochemical activation to give unsymmetrically coordinated dinuclear iron carbonyl complexes [2]. In addition, the synthesis of chiral spiro-lactams in a formal [2+2+1] cycloaddition reaction from the diazadiene derivatives, carbon monoxide and terminal alkenes was achieved regioselectively at the imine function next to the oxazine oxygen atom [3]. The mechanism of this cycloaddition reaction as well as an explanation for the observed regioselectivity was elucidated by means of high-level DFT calculations [4]. In this manuscript we will introduce highly related *N*,*N*′-(4-methyl-4*H*-1,3,4-oxadiazine-5,6-diylidene)-bis-aniline derivatives [5] into similar stoichiometric and catalytic reactions. The aim of the investigation is to see whether the same reaction principles are realized for these heterocyclic substrates that show additional functionalities compared to the substrates used in preliminary investigations. We especially wondered whether the N–N bond present in the oxadiazine ring might cause side reactions or might even be split under the reaction conditions.

2. Results and discussion

The ligands used in this investigation are *N*,*N*′-(4-methyl-4*H*-1,3,4-oxadiazine-5,6-diylidene)-bis-aniline derivatives that in addition to the exocyclic diimine unit show a heterocyclic backbone with other functional groups as the ring oxygen atom, a C=N double bond and a N–N bond. The ligands **1a**–**e** may be prepared in a three-step synthesis from bis-aryloxalimidoylchlorides (Scheme 1). The latter are reacted with methylhydrazine to produce Δ^2-1,2-diazetines that in a subsequent reaction step may be acylated with acylchlorides or anhydrides. The acylated four-membered heterocyclic compounds in a thermally induced ring enlargement reaction produce the *N*,*N*′-(4-methyl-4*H*-1,3,4-oxadiazine-5,6-diylidene)-bis-aniline derivatives [5].

Scheme 2 shows the synthesis of dinuclear iron carbonyl complexes from *N*,*N*′-(4-methyl-4*H*-1,3,4-oxadiazine-5,6-diylidene)-bis-aniline derivatives with different substituents at C_2 of the oxadiazine ring. The thermally induced reactions in *n*-heptane (50 °C) first produced an intermediate of deep bluish green colour that most probably corresponds to a mononuclear intermediate of the formula $LFe(CO)_3$ in which one iron atom symmetrically binds both imine nitrogen atoms [6]. Nevertheless, in no case these inter-

* Corresponding author. Tel.: +49 3641 948 185; fax: +49 3641 948 102.
E-mail address: Wolfgang.Imhof@uni-jena.de (W. Imhof).

0022-328X/$ - see front matter © 2009 Elsevier B.V. All rights reserved.
doi:10.1016/j.jorganchem.2009.07.024

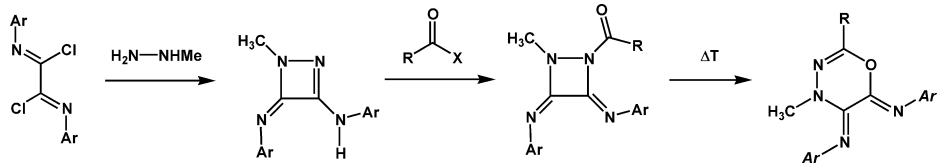

Scheme 1. Synthesis of *N*,*N*′-(4-methyl-4*H*-1,3,4-oxadiazine-5,6-diylidene)-bis-aniline derivatives [6].

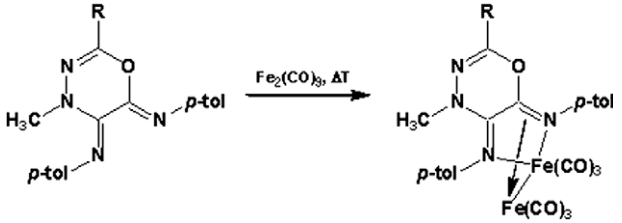

1a: R = $C(CH_3)_3$
1b: R = *p*-CH_3-C_6H_4
1c: R = CH_2CH_3
1d: R = CH_3
1e: R = CF_3

2a: R = $C(CH_3)_3$
2b: R = *p*-CH_3-C_6H_4
2c: R = CH_2CH_3
2d: R = CH_3
2e: R = CF_3

Scheme 2. Synthesis of dinuclear iron carbonyl complexes **2a**–**e**.

mediates could be isolated. During chromatographic workup albeit performed under inert conditions the colour of the product fraction turned deep red. After recrystallization of the products from light petroleum dichloromethane mixtures the molecular structure of **2a**–**e** could unequivocally be confirmed by their spectroscopic properties as well as by X-ray structure analyses of **2a**, **2b** and **2c**. Isolated yields decrease from **2a**–**e** which most probably is due to an increase of the acceptor character of the residue *R* at the heterocycle therefore reducing the ability of the oxadiazines to act as ligands.

The pattern of IR bands in the region typical for terminal carbon monoxide ligands is identical to related [$Fe_2(CO)_6$(1,4-diazabutadiene)] complexes [2]. All mass spectra show peaks corresponding to the molar masses of the complete molecules and fragmentations corresponding to the loss of CO ligands, the iron atoms and subsequent degradation of the ligands. The most significant changes in the NMR spectra of **2a**–**e** compared to the starting compounds **1a**–**e** are the ^{13}C resonances of the imine carbon atom in 6-position of the heterocycle. These signals are shifted to higher field upon coordination of both iron tricarbonyl groups to approx. 90 ppm whereas the signals of carbon atoms C_5 and C_2 of the heterocycle are observed at approx. 156 and 150 ppm, respectively. For all complexes **2a**–**e** four or three (**2b**) resonances for terminal CO ligands are observed meaning that one of the $Fe(CO)_3$ moieties rotates freely whereas the second $Fe(CO)_3$ unit is fixed. In addition, CO ligands at both iron centres do not show any interconversion on the NMR time scale.

The complexes **2a**, **2b** and **2c** could be characterized by means of X-ray diffraction (Table 1). Fig. 1 shows the molecular structure of **2a** giving the atom labelling scheme for **2a**–**c**, Table 2 summarizes the most important bond lengths and angles of all structurally characterized compounds.

Since **2a**–**c** only differ concerning the organic substituent at C1 their molecular structure is almost identical. One of the iron atoms (Fe1) symmetrically binds to both imine nitrogen atoms (N3, N4) and is situated in a co-planar fashion with respect to the diimine moiety N3–C2–C3–N4. The second iron tricarbonyl group is attached to the aforementioned plane from below displaying a metal metal bond and an additional side-on coordination towards the imine group next to the oxadiazine oxygen atom (C3–N4). From Table 2 it can be seen that the metal metal bond is slightly elongated for an aromatic substituent at C1 (**2b**) whereas the coordination of Fe2 to the imine group C3–N4 is slightly shorter for **2b** with respect to the *tert*. butyl and ethyl derivative **2a** and **2c**, respectively. In general, bond lengths and angles correspond to expected values [7].

In analogy to the related proline based diazadiene substrates oxadiazines **1a**–**e** produce chiral spiro-lactams **3a**–**e** as a result of a formal [2+2+1] cycloaddition reaction of one of the exocyclic imine functions with carbon monoxide and ethylene in the presence of catalytic amounts of $Ru_3(CO)_{12}$ [2]. Yields of **3a**–**e** decrease in the same order as it has been observed for the formation of the dinuclear iron carbonyl complexes **2a**–**e** leading to only trace amounts of **3d** and **3e** whereas **3a**–**c** could be purified and fully characterized. In connection with our DFT calculations on the mechanism of this type of cycloaddition reaction it has been pointed out that compounds of the general formula $LM(CO)_3$ (M = Fe, Ru) are both the catalytically active species in the cycloaddition reaction and the intermediates in the synthesis of compounds of type **2** [3]. So obviously the same electronic effects that lead to a diminished yield in the order **2a**–**e** by hampering the attack of another $Fe(CO)_3$ moiety from the basis of square-pyramidal $LFe(CO)_3$ also prevent the approach of ethylene from the same direction which has been shown to be the rate determining step of the catalytic cycloaddition [3].

Interestingly, the NMR spectra of **3a**–**c** show a strong temperature dependence thus indicating dynamic processes. In Fig. 2 ^{13}C

Table 1
Crystal data and refinement details for the X-ray structure determinations of **2a**, **2b** and **2c**.

	2a	2b	2c
Formula	$C_{28}H_{26}Fe_2N_4O_7$	$C_{31}H_{24}Fe_2N_4O_7$	$C_{26}H_{22}Fe_2N_4O_7$
Formula weight (g mol^{-1})	642.24	676.13	614.17
T (K)	183(2)	183(2)	183(2)
Crystal system	monoclinic	triclinic	triclinic
Space group	$P2_1/n$	$P\bar{1}$	$P\bar{1}$
a (Å)	11.2473(4)	9.6469(9)	8.6009(2)
b (Å)	17.6247(4)	11.9331(9)	10.8307(3)
c (Å)	16.0443(7)	14.682(1)	15.6246(5)
α (°)	90	77.431(4)	106.265(2)
β (°)	109.574(2)	72.101(5)	96.666(2)
γ (°)	90	72.540(5)	95.382(2)
Volume (Å^3)	2996.7(2)	1519.6(2)	1375.56(7)
Z	4	2	2
ρ_{calc} [g cm^{-3}]	1.424	1.478	1.483
μ (cm^{-1})	10.18	10.08	11.05
Measured data	20 969	8845	9875
Unique data	6827	6240	6238
R_{int}	0.0688	0.0288	0.0235
Data with $I > 2\sigma(I)$	4495	4919	5001
Number of parameters	376	401	356
wR_2 (all data, on F^2)[a]	0.1045	0.1475	0.0956
$R_1(I > 2\sigma(I))$[a]	0.0423	0.0516	0.0367
Goodness-of-fit[b]	0.956	1.019	1.002
Res. dens. (e Å^{-3})	0.377/−0.482	0.524/−0.797	0.842/−0.409

[a] Definition of the *R* indices: $R_1 = (\sum||F_o| - |F_c||)/\sum|F_o|$, $wR_2 = \sum[w(F_o^2 - F_c^2)^2]/\sum[w(F_o^2)^2]^{1/2}$ with $w^{-1} = \sigma^2(F_o^2) + (aP)^2$.
[b] GOF $= \sum[w(F_o^2 - F_c^2)^2]/(N_o - N_p)^{1/2}$.

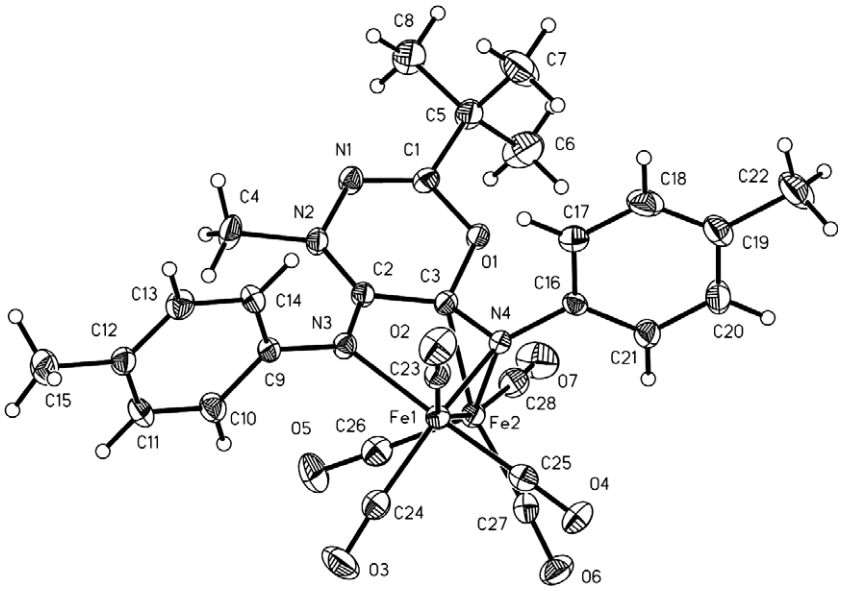

Fig. 1. Molecular structure of **2a**.

Table 2
Selected bond lengths (pm) and angles (°)..

	2a	2b	2c		2a	2b	2c
Fe1–N4	195.1(2)	196.7(2)	196.1(2)	N1–N2	141.1(3)	140.8(3)	140.7(3)
Fe1–N3	202.1(2)	202.6(2)	202.7(2)	N2–C2	134.2(3)	134.9(4)	134.6(3)
Fe1–Fe2	256.79(6)	258.92(6)	256.43(4)	N2–C4	146.3(3)	146.2(4)	146.1(3)
Fe2–N4	192.4(2)	191.4(2)	193.5(2)	N3–C2	130.7(3)	130.5(4)	130.4(3)
Fe2–C3	201.1(3)	199.4(3)	201.0(2)	N4–C3	139.3(3)	139.5(4)	139.0(3)
O1–C1	135.7(3)	136.6(3)	135.9(3)	C1–C5	150.5(4)	147.1(4)	149.6(3)
O1–C3	140.4(3)	142.7(4)	140.8(3)	C2–C3	147.7(4)	147.7(4)	147.0(3)
N1–C1	126.7(3)	128.3(4)	126.8(3)				
N4–Fe1–N3	84.11(9)	83.9(1)	83.60(7)	Fe2–N4–Fe1	83.00(8)	83.7(1)	82.31(7)
N4–Fe1–Fe2	48.04(7)	47.27(7)	48.40(5)	N1–C1–O1	126.0(2)	123.9(3)	125.7(2)
N3–Fe1–Fe2	86.08(6)	88.24(7)	86.53(5)	N1–C1–C5	122.5(3)	120.4(3)	122.4(2)
N4–Fe2–C3	41.4(1)	41.8(1)	41.22(8)	O1–C1–C5	111.5(2)	115.6(2)	111.9(2)
N4–Fe2–Fe1	48.96(6)	49.04(7)	49.29(5)	N3–C2–N2	130.6(2)	130.1(2)	129.9(2)
C3–Fe2–Fe1	71.21(8)	70.86(8)	71.35(6)	N3–C2–C3	113.0(2)	113.9(2)	113.4(2)
C1–O1–C3	117.9(2)	113.4(2)	115.9(2)	N2–C2–C3	116.2(2)	116.0(2)	116.5(2)
C1–N1–N2	118.2(2)	117.0(2)	118.8(2)	N4–C3–O1	114.4(2)	115.0(2)	114.2(2)
C2–N2–N1	121.5(2)	121.1(2)	121.3(2)	N4–C3–C2	117.3(2)	116.4(2)	117.2(2)
C2–N2–C4	126.5(2)	127.0(3)	127.1(2)	O1–C3–C2	115.9(2)	113.9(2)	116.2(2)
N1–N2–C4	111.7(2)	111.7(2)	111.5(2)	N4–C3–Fe2	66.0(1)	66.0(2)	66.5(1)
C2–N3–Fe1	112.5(2)	111.6(2)	112.2(1)	O1–C3–Fe2	115.9(2)	120.0(2)	120.0(2)
C3–N4–Fe2	72.7(2)	72.2(2)	72.3(1)	C2–C3–Fe2	113.3(2)	117.2(2)	113.6(2)
C3–N4–Fe1	106.7(2)	105.7(2)	106.4(1)				

NMR spectra of **3a** at 223, 300 and 323 K are depicted together with the assignment of resonances to respective carbon atoms (derived from HMBC/HQMC experiments). It clearly demonstrates that at lower temperature two sets of signals are observed whereas at 323 K only one set of signals representing the averaged structure is visible. At 300 K a broadening of signals appears indicating that coalescence occurs near room temperature. The carbon atoms that are highly affected by this dynamic process are the nitrogen bound methyl group (4), the quarternary carbon atom of the unreacted imine function (5) and one of the CH functions of one of the tolyl substituents (16). We therefore interpret these observations as a *E*-/*Z*-interconversion of the unreacted imine moiety due to relatively strong interactions between the methyl group and the tolyl imine substructure (Scheme 3). In the *Z*-isomer the tolyl substituent of the imine group interfers with the NMe function whereas there should be no interaction in the *E*-isomer. The free activation enthalpy of this equilibrium of **3a** may be calculated from the resonances of carbon atoms 4, 5 and 16 (Fig. 2) and shows a value of 58.7(3) kJ mol^{-1} [8].

The ^{13}C NMR spectra at different temperatures therefore also clarify the regioselectivity of the catalytic reaction itself. Since there is only one resonance for the spiro carbon atom at 94.16 ppm (Fig. 2, 323 K) the reaction proceeds regioselectively at the imine function next to the oxadiazine oxygen atom. The imine group at the 5-position of the oxadiazine core remains unreacted during the catalytic cycle.

3. Experimental

All procedures were carried out under an argon atmosphere in anhydrous, freshly distilled solvents. The syntheses of the oxadiazine derivatives **1a**–**e** were performed following a literature

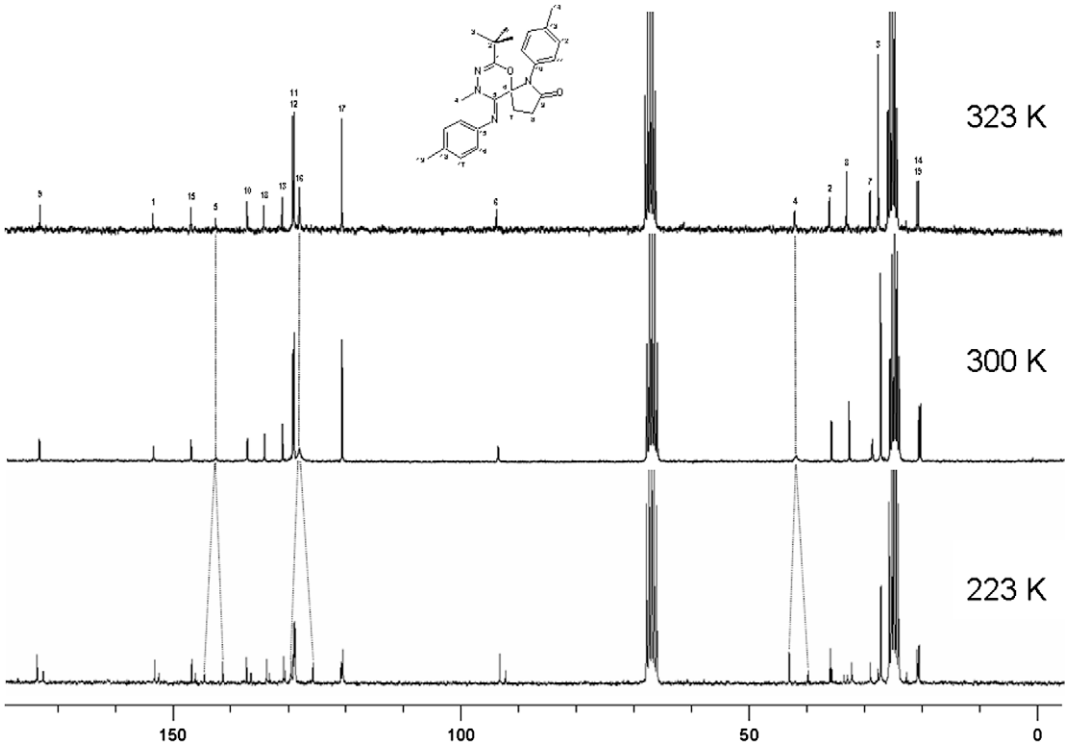

Fig. 2. ^{13}C NMR spectra of **3a** at different temperatures.

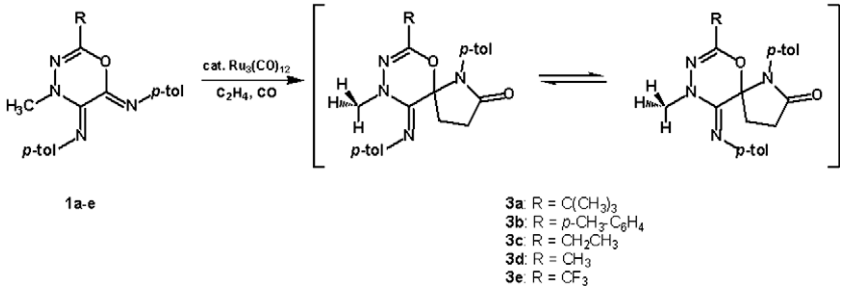

Scheme 3. Formation of chiral spiro-lactams **3a–e**.

method [5]. Infrared spectra were recorded on a Perkin Elmer FT-IR System 2000 using 0.2 mm KBr cuvettes. NMR spectra were recorded on a Bruker DRX 400 spectrometer (^1H: 400.13 MHz, ^{13}C: 100.62 MHz, solvent as internal standard). Mass spectra were recorded on a Finnigan MAT SSQ 710 instrument. Elemental analyses were carried out at the laboratory of the Institute of Organic Chemistry and Macromolecular Chemistry of the Friedrich–Schiller-University Jena.

3.1. X-ray structure determinations

Intensity data were collected on a Nonius Kappa CCD diffractometer using graphite-monochromated Mo Kα radiation. Data were corrected for Lorentz polarization but not for absorption effects [9,10]. Crystallographic data as well as structure solution and refinement details are summarized in Table 1. The structures were solved by direct methods (SHELXS) and refined by full-matrix least squares techniques against Fo^2 (SHELXL-97) [11,12]. The hydrogen atoms were included at calculated positions with fixed thermal parameters. All non-hydrogen atoms were refined anisotropically. XP (SIEMENS Analytical X-ray Instruments, Inc.) was used for structure representations.

3.2. Synthesis of ***2a–e***

A 0.685 mmol (0.25 g) sample of $Fe_2(CO)_9$ was stirred together with 0.825 mmol of the corresponding ligand (**1a**: 0.299 g, **1b**: 0.327 g, **1c**: 0.276 g, **1d**: 0.264 g, **1e**: 0.309 g) in 20 ml of *n*-heptane at 50 °C for 2 h. The yellow suspension turned blueish-green. The solvent was evaporated in vacuo and the solid residue was dissolved in 2 ml of CH_2Cl_2. 200 mg of silanized silica gel was added and the solvent was again evaporated. Chromatography using a mixture of light petroleum (b.p. 40–60 °C) and CH_2Cl_2 as the eluent with increasing polarity yielded **2a–e** as deep red solutions. After the solvents were evaporated the crude products were recrystallized from a mixture of light petroleum (b.p. 40–60 °C) and CH_2Cl_2 at −20 °C. Yields: **1a**: 222 mg (50.5%), **1b**: 191 mg (41.2%), **1c**: 141 mg (33.5%), **1d**: 126 mg (30.7%), **1e**: 132 mg (29.5%).

3.2.1. MS and spectroscopic data for ***2a***

MS (FAB) [*m/z* (%)]: 643 (1) [MH^+], 627 (2) [M^+−Me], 614 (2) [M^+−CO], 586 (10) [M^+−2CO], 571 (2) [M^+−Me−2CO], 558 (6) [M^+−3CO], 530 (12) [M^+−4CO], 507 (8) [M^+−5CO], 474 (5) [M^+−6CO], 446 (8) [M^+−5CO−Fe], 418 (20) [M^+−6CO−Fe], 363 (100) [MH^+−6CO−2Fe], 258 (20) [LH^+−C_7H_7N], 230 (22)

[$LH^+-C_8H_7NO$]; IR (Nujol, 298 K) [cm^{-1}]: 2059, 2008, 1975, 1943, 1921 (vs, ν(CO)); 1655 (w, ν(C=N)); 1595 (s, ν(C=C)); 1508 (w, ν(C=C)); ^{1}H NMR (400 MHz, THF-d^8, 298 K) [ppm]: 0.94 (s, 9H, CH_3 (^{t}Bu)), 2.30 (s, 3H, Ph–CH_3), 2.37 (s, 3H, Ph–CH_3), 2.58 (s, 3H, N–CH_3), 6.96 (m, 2H, CH_{Ph}), 7.18 (m, 4H, CH_{Ph}), 7.45 (m, 2H, CH_{Ph}); ^{13}C NMR (400 MHz, THF-d^8, 298 K) [ppm]: 20.9 (Ph-CH_3), 27.3 (CH_3(^{t}Bu)), 36.2 (^{q}C(^{t}Bu)), 42.8 (N-CH_3), 90.5 (C=N), 124.7 (CH_{Ph}), 125.2 (CH_{Ph}), 126.8 (CH_{Ph}), 130.1 (CH_{Ph}), 130.4 (CH_{Ph}), 136.7 (^{q}C$_{Ph}$), 137.0 (^{q}C$_{Ph}$), 147.1 (^{q}C$_{Ph}$), 150.5 (^{q}C$_{Ph}$), 155.7 (N=C–^{t}Bu), 155.9 (C=N), 202.8 (CO), 210.5 (CO), 214.5 (CO), 217.7 (CO); Anal. Calc. for $C_{28}H_{26}N_4O_7Fe_2$: C, 52.34; H, 4.05; N, 8.72. Found: C, 51.27; H, 4.50; N, 8.52%.

3.2.2. MS and spectroscopic data for **2b**

MS (DEI) [*m/z* (%)]: 648 (1) [M^+−CO], 620 (3) [M^+−2CO], 592 (2) [M^+−3CO], 564 (13) [M^+−4CO], 536 (15) [M^+−5CO], 508 (11) [M^+−6CO], 480 (9) [M^+−5CO−Fe], 452 (25) [M^+−6CO−Fe], 396 (56) [M^+−6CO−2Fe], 279 (39) [$L^+-C_8H_7N$], 146 (37) [$C_9H_{10}N_2^+$], 119 (100) [C_8H_7O], 91 (65) [$C_7H_7^+$]; IR (Nujol, 298 K) [cm^{-1}]: 2063, 2007, 1994, 1981, 1933 (vs, ν(CO)); 1628 (w, ν(C=N)); 1594 (m, ν(C=C)); 1505 (w, ν(C=C)); 1401(w, ν(C=C)); ^{1}H NMR (400 MHz, THF-d^8, 298 K) [ppm]: 2.28 (s, 3H, Ph–CH_3), 2.33 (s, 3H, Ph–CH_3), 2.39 (s, 3H, Ph–CH_3), 2.75 (s, 3H, N–CH_3), 6.98 (m, 2H, CH_{Ph}), 7.07 (m, 2H, CH_{Ph}), 7.19 (m, 2H, CH_{Ph}), 7.24 (m, 2H, CH_{Ph}), 7.42 (m, 2H, CH_{Ph}), 7.54 (m, 2H, CH_{Ph}); ^{13}C NMR (200 MHz, THF-d^8, 298 K) [ppm]: 20.9 (Ph-CH_3), 20.9 (Ph-CH_3), 21.3 (Ph-CH_3), 43.2 (N-CH_3), 91.0 (C=N), 124.8 (CH_{Ph}), 125.0 (CH_{Ph}), 126,4 (^{q}C$_{Ph}$), 126.7 (CH_{Ph}), 126.8 (CH_{Ph}), 129.6 (CH_{Ph}), 130.1 (CH_{Ph}), 130.4 (CH_{Ph}), 130.5 (CH_{Ph}), 136.8 (^{q}C$_{Ph}$), 137.1 (^{q}C$_{Ph}$), 142.2 (^{q}C$_{Ph}$), 146.9 (^{q}C$_{Ph}$), 147.1 (^{q}C$_{Ph}$), 150.5 (N=C–Ph), 156.8 (C=N), 210.6 (CO), 214.4 (CO), 217.6 (CO); Anal. Calc. for $C_{31}H_{24}N_4O_7Fe_2$: C, 55.03; H, 3.55; N, 8.28. Found: C, 54.87; H, 3.62; N, 7.93%.

3.2.3. MS and spectroscopic data for **2c**

MS (DEI) [*m/z* (%)]: 586 (1) [M^+−CO], 558 (1) [M^+−2CO], 530 (1) [M^+−3CO], 502 (1) [M^+−4CO], 474 (1) [M^+−5CO], 446 (1) [M^+−6CO], 418 (1) [M^+−5CO−Fe], 390 (1) [M^+−6CO−Fe], 334 (4) [M^+−6CO−2Fe], 319 (3) [L^+-CH_3], 243 (11) [$L^+-C_7H_7$], 217 (100) [L^+-C_8H_7N]; IR (Nujol, 298 K) [cm^{-1}]: 2058, 2007, 1976, 1935 (s, ν(CO)); 1682 (w, ν(C=N)); 1584 (m, ν(C=C)), 1504 (m, ν(C=C)). ^{1}H NMR (400 MHz, THF-d^8, 298 K) [ppm]: 1.29 (br, 3H, CH_3), 2.06 (br, 2H, CH_2), 2.30 (s, 3H, Ph-CH_3), 2.37 (s, 3H, Ph-CH_3), 2.59 (s, 3H, N-CH_3), 6.96 (m, 2H, CH_{Ph}), 7.18 (m, 4H, CH_{Ph}), 7.43 (m, 2H, CH_{Ph}); ^{13}C NMR (400 MHz, THF-d^8, 298 K) [ppm]: 9.8 (CH_3), 20.8 (Ph-CH_3), 20.9 (Ph-CH_3), 30.5 (CH_2), 42.7 (N-CH_3), 90.5 (C=N), 124.8 (CH_{Ph}), 125.1 (CH_{Ph}), 126.5 (CH_{Ph}), 130.1 (CH_{Ph}), 130.4 (CH_{Ph}), 136.6 (^{q}C$_{Ph}$), 137.0 (^{q}C$_{Ph}$), 147.0 (^{q}C$_{Ph}$), 150.5 (^{q}C$_{Ph}$), 152.1 (N=C–Et), 156.7 (C=N), 202.8 (CO), 210.4 (CO), 214.4 (CO), 217.5 (CO); Anal. Calc. for $C_{26}H_{22}N_4O_7Fe_2$: C, 50.81; H, 3.58; N, 9.12. Found: C, 50.32; H, 4.01; N, 8.65%.

3.2.4. MS and spectroscopic data for **2d**

MS (DEI) [*m/z* (%)]: 600 (1) [M^+], 572 (13) [M^+−CO], 544 (20) [M^+−2CO], 516 (14) [M^+−3CO], 488 (50) [M^+−4CO], 460 (100) [M^+−5CO], 432 (50) [M^+−6CO], 404 (25) [M^+−5CO−Fe], 376 (92) [M^+−6CO−Fe], 320 (28) [M^+−6CO−2Fe], 216 (30) [$LH^+-C_7H_7N$], 203 (21) [$L^+-C_7H_7NC$], 146 (13) [$C_9H_{10}N_2^+$], 91 (13) [$C_7H_7^+$]; IR (Nujol, 298 K) [cm^{-1}]: 2055, 2011, 1990, 1982, 1962, 1939, 1926 (vs, ν(CO)); 1670 (w, ν(C=N)); 1589 (m, ν(C=C)); 1504 (m, ν(C=C)); ^{1}H NMR (400 MHz, THF-d^8, 298 K) [ppm]: 1.30 (s, 3H, N=–CH_3), 2.30 (s, 3H, Ph–CH_3), 2.38 (s, 3H, Ph–CH_3), 2.59 (s, 3H, N–CH_3), 6.94 (m, 2H, CH_{Ph}), 7.19 (m, 4H, CH_{Ph}), 7.43 (m, 2H, CH_{Ph}); ^{13}C NMR (400 MHz, THF-d^8, 298 K) [ppm]: 17.1 (CH_3), 20.8 (Ph-CH_3), 42.6 (N-CH_3), 90.7 (C=N), 124.8 (CH_{Ph}), 125.1 (CH_{Ph}), 126.5 (CH_{Ph}), 130.2 (CH_{Ph}), 130.4 (CH_{Ph}), 130.5 (CH_{Ph}), 136.6 (^{q}C$_{Ph}$), 137.0 (^{q}C$_{Ph}$), 146.9 (^{q}C$_{Ph}$), 149.1 (^{q}C$_{Ph}$), 150.5 (N=C–Me), 156.8 (C=N), 203.1 (CO), 210.6 (CO), 214.6 (CO), 217.9 (CO); Anal. Calc. for $C_{25}H_{20}N_4O_7Fe_2$: C, 50.00; H, 3.33; N, 9.33. Found: C, 49.39; H, 3.59; N, 8.92%.

3.2.5. MS and spectroscopic data for **2e**

MS (DEI) [*m/z* (%)]: 654 (1) [M^+], 626 (2) [M^+−CO], 598 (3) [M^+−2CO], 570 (1) [M^+−3CO], 542 (7) [M^+−4CO], 514 (6) [M^+−5CO], 486 (3) [M^+−6CO], 458 (2) [M^+−5CO−Fe], 430 (7) [M^+−6CO−Fe], 374 (7) [M^+−6CO−2Fe], 355 (23) [L^+-F], 341 (14) [LH^+–F–CH_3], 281 (73) [$C_{11}H_7F_3FeNO^+$], 221 (96) [$C_{11}H_9F_2N_3^+$], 207 (100) [$C_{10}H_7F_2N_3^+$], 173 (44) [$C_{10}H_{10}N_3^+$]; IR (Nujol, 298 K) [cm^{-1}]: 2059, 2020, 1992, 1969, 1939 (vs, ν(CO)); 1684 (w, ν(C=N)); 1589 (m, ν(C=C)); 1502 (m, ν(C=C)); 1156 (m, ν(C–F)); ^{1}H NMR (400 MHz, THF-d^8, 298 K) [ppm]: 2.32 (s, 3H, Ph–CH_3), 2.38 (s, 3H, Ph-CH_3), 2.69 (s, 3H, N–CH_3), 6.99 (m, 2H, CH_{Ph}), 7.21 (m, 4H, CH_{Ph}), 7.47 (m, 2H, CH_{Ph}); ^{13}C NMR (400 MHz, THF-d^8, 298 K) [ppm]: 20.8 (Ph-CH_3), 20.9 (Ph-CH_3), 43.7 (N-CH_3), 91.2 (C=N), 117.4 (q, CF_3, $^1J_{CF}$ = 274 Hz), 124.2 (CH_{Ph}), 124.5 (CH_{Ph}), 126.3 (CH_{Ph}), 130.3 (CH_{Ph}), 130.7 (CH_{Ph}), 137.2 (^{q}C$_{Ph}$), 137.5 (q, N=C–CF_3, $^2J_{CF}$ = 41 Hz), 137.9 (^{q}C$_{Ph}$), 146.0 (^{q}C$_{Ph}$), 149.7 (^{q}C$_{Ph}$), 156.5 (C=N), 202.4 (CO), 210.0 (CO), 213.6 (CO), 217.2 (CO); Anal. Calc. for $C_{25}H_{17}N_4O_7Fe_2$: C, 45.87; H, 2.60; N, 8.56. Found: C, 46.39; H, 2.89; N, 8.08%.

3.3. Synthesis of **3a–e**

About 0.25 mmol of the corresponding *N*,*N*′-(4-methyl-4*H*-1,3,4-oxadiazine-5,6-diylidene)bis(4-methylaniline) (for **3a**: 91 mg, **3b**: 99 mg, **3c**: 84 mg, **3d**: 80 mg, **3e**: 94 mg) were transferred together with 0.01 mmol (26 mg) $Ru_3(CO)_{12}$ into a 75 ml stainless steel autoclave. After evaporation of the autoclave, 3 ml of toluene were added under an argon atmosphere. Afterwards the autoclave was pressurized with 12 atm CO and 8 atm ethylene and the reaction mixture was heated to 140 °C for 16 h or 3d, respectively. After the autoclave was cooled down to room temperature the pressure was released and the solution transferred into a Schlenk tube. After evaporation of toluene a brown oily residue was obtained. This residue was used to determine the conversion of the educt by NMR spectroscopy. In the case of **3a–d** products were purified by HPLC using pentane/methanol (**3a**, **3b**) or pentane/THF mixtures (**3c**, **3d**) as eluent. Yields: **3a**: 61 mg (58%), **3b**: 70 mg (62%), **3c**: 51 mg (52%), **3d**: 13 mg (14%). In case of **3e** conversion rates were too low to allow purification by HPLC methods (see Table 3).

3.3.1. MS and spectroscopic data for **3a**

MS (DEI): *m/z* (%) = 418 (100) [M^+], 361 (13) [M^+−C(CH_3)$_3$], 312 (24) [$M^+-C_7H_7NH$], 290 (48) [$C_{19}H_{18}N_2O^+$], 262 (40) [$C_{18}H_{18}N_2^+$], 247 (12) [$C_{17}H_{15}N_2^+$], 233 (2) [$C_{16}H_{13}N_2^+$], 144 (26) [$C_{10}H_{10}N^+$], 117 (11) [$C_8H_7N^+$], 91 (16) [$C_7H_7^+$]; IR (Nujol, 298 K) [cm^{-1}]: 3021 (w, ν(CH_{Ar})), 2969 (w, ν_{as}(CH_3)), 2918 (w, ν_{as}(CH_2)), 2874 (w, ν_s(CH_2)), 1722 (s, ν(C=O)), 1632 (s, ν(C=N)), 1513 (m, ν(C=C)), 1458 (w, δ(CH_2)), 1164, 1142 (s, ν_{as}(C–O–C)); ^{1}H NMR (200 MHz, THF-d^8, 323 K) [ppm]: 1.15 (s, 9H, CH_3 (^{t}Bu)), 2.23 (s,

Table 3
Conversion of **1a–e** and isolated yields of **3a–e** after HPLC.

Compound	Conversion after 16 h (%)	Conversion after 3 day (%)	Isolated yields (%)
3a	≈100		58
3b	45	>95	62
3c	n.d.	>95	52
3d	45	20	14
3e	6	7	

3H, Ph-CH_3), 2.31 (s, 3H, Ph–CH_3), 2.09–2.39 (m, 1H, CH_2), 2.49–2.67 (m, 2H, CH_2), 2.79 (s, 3H, N–CH_3), 2.86–2.97 (m, 1H, CH_2), 6.47 (m, 2H, CH_{Ph}), 6.95 (m, 2H, CH_{Ph}), 7.14 (m, 4H, CH_{Ph}); ^{13}C NMR (50 MHz, THF-d^8, 323 K) [ppm]: 20.6 (Ph–CH_3), 20.9 (Ph-CH_3), 27.7 (CH_3 (^tBu)), 29.1 (CH_2), 33.2 (CH_2), 36.1 (^qC (^tBu)), 42.2 (N-CH_3), 94.1 (^{sp}C), 121.0 (CH_{Ph}), 128.4 (CH_{Ph}), 129.3 (CH_{Ph}), 129.5 (CH_{Ph}), 131.4 ($^qC_{Ph}$), 134.6 ($^qC_{Ph}$), 137.5 ($^qC_{Ph}$), 143.0 (C=N), 147.3 ($^qC_{Ph}$), 153.9 (N=C–^tBu), 173.5 (C=O); Anal. Calc. for $C_{25}H_{30}N_4O_2$: C, 71.77; H, 7.18; N, 13.40. Found: C, 70.68; H, 7.22; N, 13.16%.

3.3.2. MS and spectroscopic data for ***3b***

MS (DEI): *m/z* (%) = 452 (84) [M^+], 346 (23) [M^+-C_7H_7NH], 320 (16) [$C_{20}H_{22}N_3O^+$], 290 (76) [$C_{19}H_{18}N_2O^+$], 275 (38) [$C_{18}H_{15}N_2O^+$], 262 (50) [$C_{18}H_{18}N_2^+$], 247 (18) [$C_{17}H_{15}N_2^+$], 163 (14) [$C_9H_{11}N_2O^+$], 146 (69) [$C_9H_{10}N_2^+$], 119 (95) [$C_8H_7O^+$], 107 (70) [$C_7H_7O^+$], 91 (100) [$C_7H_7^+$]; IR (Nujol, 298 K) [cm^{-1}]: 3035 (w, $\nu(CH_{Ar})$), 2922 (w, $\nu_{as}(CH_2)$), 2856 (w, $\nu_s(CH_2)$), 1719 (s, ν(C=O)), 1625 (s, ν(C=N)), 1606 (s, ν(C=C)), 1449 (m, $\delta(CH_2)$), 1211 (s, ν_{as}(C–O–C)); ^1H NMR (400 MHz, THF-d^8, 323 K) [ppm]: 2.25, 2.26 (2s, 6H, Ph-CH_3), 2.35 (s, 3H, Ph–CH_3), 2.22–3.33 (m, 1H, CH_2), 2.64–2.75 (m, 2H, CH_2), 2.81 (s, 3H, N-CH_3), 3.16–3.25 (m, 1H, CH_2), 6.61 (m, 2H, CH_{Ph}), 7.03 (m, 6H, CH_{Ph}), 7.18 (m, 2H, CH_{Ph}), 7.65 (m, 2H, CH_{Ph}); ^{13}C NMR (100 MHz, THF-d^8, 323 K) [ppm]: 20.6 (Ph-CH_3), 20.9 (Ph-CH_3), 21.2 (Ph-CH_3), 29.1 (CH_2), 32.5 (CH_2), 42.5 (N–CH_3), 94.2 (^{sp}C), 121.1 (CH_{Ph}), 126.4 (CH_{Ph}), 128.8 (CH_{Ph}), 129.0 ($^qC_{Ph}$), 129.2 ($^qC_{Ph}$), 129.5 (CH_{Ph}), 129.6 (CH_{Ph}), 129.7 (CH_{Ph}), 131.8 ($^qC_{Ph}$), 134.3 ($^qC_{Ph}$), 138.2 ($^qC_{Ph}$), 140.9 ($^qC_{Ph}$), 145.1 (C=N–Ar), 147.2 (C=N–Ar), 173.7 (C=O); Anal. Calc. for $C_{28}H_{29}N_4O_2$: C, 74.17; H, 6.40; N, 12.36. Found: C, 73.52; H, 6.54; N, 11.90%.

3.3.3. MS and spectroscopic data for ***3c***

MS (DEI): *m/z* (%) = 390 (100) [M^+], 320 (10) [$C_{20}H_{21}N_3OH^+$], 290 (23) [$C_{19}H_{18}N_2O^+$], 275 (14) [$C_{18}H_{15}N_2O^+$], 262 (15) [$C_{18}H_{18}N_2^+$], 247 (6) [$C_{17}H_{15}N_2^+$], 217 (31) [$C_{12}H_{15}N_3O^+$], 146 (15) [$C_9H_8NO^+$], 107 (20) [$C_5H_3N_2O^+$], 91 (12) [$C_7H_7^+$]; IR (Nujol, 298 K) [cm^{-1}]: 3030 (w, $\nu(CH_{Ar})$), 2940 (w, $\nu_{as}(CH_3)$), 2925 (w, $\nu_{as}(CH_2)$), 2872 (w, $\nu_s(CH_3)$), 1720 (m, ν(C=O)), 1633 (s, ν(C=N)), 1606 (s, ν(C=C)), 1450 (m, $\delta(CH_2)$), 1201 (s, ν_{as}(C–O–C)); ^1H NMR (400 MHz, THF-d^8, 323 K) [ppm]: 1.00 (t, 3H, CH_3), 1.13 (t, 3H, CH_3), 2.24 (s, 3H, Ph-CH_3), 2.31 (s, 3H, Ph-CH_3), 2.14–2.37 (m, 4H, CH_2), 2.46–2.55 (m, 1H, CH_2), 2.72 (s, 3H, N–CH_3), 3.09 (m, 1H, CH_2), 6.56 (m, 2H, CH_{Ph}), 7.00 (m, 4H, CH_{Ph}), 7.45 (m, 2H, CH_{Ph}); ^{13}C NMR (100 MHz, THF-d^8, 323 K) [ppm]: 9.7 (CH_3), 10.0 (CH_3), 20.6 (Ph-CH_3), 21.0 (Ph-CH_3), 25.7 (N=C–CH_2), 26.0 (N=C–CH_2), 29.1 (CH_2), 30.5 (CH_2), 32.8 (CH_2), 42.0 (N–CH_3), 94.0 (^{sp}C), 119.8 ($^qC_{Ph}$), 121.1 (CH_{Ph}), 128.9 (CH_{Ph}), 129.5 (CH_{Ph}), 129.6 (CH_{Ph}), 131.5 ($^qC_{Ph}$), 134.4 ($^qC_{Ph}$), 138.2 (C=N), 138.3 (C=N), 147.4 ($^qC_{Ph}$), 149.4 (C=N), 173.5 (C=O); Anal. Calc. for $C_{23}H_{26}N_4O_2$: C, 70.77; H, 6.67; N, 14.36. Found: C, 70.08; H, 6.56; N, 14.06%.

3.3.4. MS and spectroscopic data for ***3d***

MS (DEI): *m/z* (%) = 376 (17) [M^+], 335 (3) [MH^+–CO–CH_2], 290 (5) [$C_{19}H_{18}N_2O^+$], 262 (5) [$C_{18}H_{18}N_2^+$], 246 (49) [$C_{13}H_{16}N_3O_2^+$], 232 (13) [$C_{13}H_{17}N_3OH^+$], 203 (19) [$C_{11}H_{13}N_3O^+$], 149 (63) [$C_9H_{10}NOH^+$], 133 (32) [$C_7H_7NCO^+$], 117 (26) [$C_7H_7NC^+$], 107 (100) [$C_5H_3N_2O^+$], 91 (35) [$C_7H_7^+$]; IR (Nujol, 298 K) [cm^{-1}]: 3028 (w, $\nu(CH_{Ar})$), 2975 (w, $\nu_{as}(CH_3)$), 2922 (w, $\nu_{as}(CH_2)$), 2858 (w, $\nu_s(CH_2)$), 1716 (s, ν(C=O)), 1624 (s, ν(C=N)), 1606 (s, ν(C=C)), 1445 (m, $\delta(CH_2)$), 1212 (s, ν_{as}(C–O–C)); ^1H NMR (400 MHz, THF-d^8, 323 K) [ppm]: 1.82 (s, 3H, CH_3), 2.23 (s, 3H, Ph–CH_3), 2.31 (s, 3H, Ph-CH_3), 2.14–2.38 (m, 2H, CH_2), 2.46–2.52 (m, 1H, CH_2), 2.68 (s, 3H, N–CH_3), 3.13–3.16 (m, 1H, CH_2), 6.57 (m, 2H, CH_{Ph}), 6.97 (m, 2H, CH_{Ph}), 7.12 (m, 4H, CH_{Ph}); ^{13}C NMR (100 MHz, THF-d^8, 323 K) [ppm]: 18.0 (CH_3), 20.6 (Ph-CH_3), 21.0 (Ph–CH_3), 29.1 (CH_2), 32.7 (CH_2), 41.9 (N–CH_3), 94.0 (^{sp}C), 119.2 ($^qC_{Ph}$), 121.1 (CH_{Ph}), 129.0 (CH_{Ph}), 129.6 (CH_{Ph}), 129.7 (CH_{Ph}), 131.5 ($^qC_{Ph}$), 134.4 ($^qC_{Ph}$), 138.4 ($^qC_{Ph}$), 145.9 (C=N), 147.4 (C=N), 173.5 (C=O); Anal. Calc. for $C_{22}H_{24}N_4O_2$: C, 70.21; H, 6.38; N, 14.89. Found: C, 69.84; H, 6.86; N, 14.27%.

3.3.5. MS and spectroscopic data for ***3e***

MS (DEI): *m/z* (%) = 430 (1) [M^+], 402 (1) [M^+–CO], 335 (2) [$C_{20}H_{21}N_3O_2^+$].

Appendix A. Supplementary material

CCDC 725446, 725447 and 725448 contain the supplementary crystallographic data for **2a**, **2b** and **2c** in this paper. These data can be obtained free of charge from The Cambridge Crystallographic Data Centre via www.ccdc.cam.ac.uk/data_request/cif.

Supplementary data associated with this article can be found, in the online version, at doi:10.1016/j.jorganchem.2009.07.024.

References

[1] (a) For recent reviews see: J.A. Varela, C. Saa, Synlett (2008) 2571;
(b) D.K. Rayabarapu, C.-H. Cheng, Acc. Chem. Res. 40 (2007) 971;
(c) B. Heller, M. Hapke, Chem. Soc. Rev. 36 (2007) 1085;
(d) T. Shibata, Adv. Synth. Catal. 348 (2006) 2328;
(e) P.R. Chopade, J. Louie, Adv. Synth. Catal. 348 (2006) 2307;
(f) G. Vasapollo, G. Mele, Curr. Org. Chem. 10 (2006) 1397;
(g) S. Kotha, E. Brahmachary, K. Lahiri, Eur. J. Org. Chem. (2005) 4741;
(h) S. Agarwal, S. Cämmerer, S. Filali, W. Fröhner, J. Knöll, M.P. Krahl, K.R. Reddy, H.-J. Knölker, Curr. Org. Chem. 9 (2005) 1601;
(i) D. Strübing, M. Beller, in: M. Beller, C. Bolm (Eds.), Transition Metals for Organic Synthesis, second ed., vol. 1, Wiley-VCH, Weinheim, Germany, 2004, p. 619;
(j) S.E. Gibson, N. Mainolfi, Angew. Chem., Int. Ed. 44 (2005) 3022;
(k) N. Chatani, Chem. Rec. 8 (2008) 201.
[2] W. Imhof, A. Göbel, R. Beckert, T. Billert, J. Organomet. Chem. 590 (1999) 104.
[3] (a) A. Göbel, W. Imhof, J. Chem. Soc., Chem. Commun. (2001) 593;
(b) A. Göbel, W. Imhof, J. Mol. Catal. A: Chem. 197 (1–2) (2003) 15.
[4] (a) W. Imhof, E. Anders, A. Göbel, H. Görls, Chem. Eur. J. 9 (2003) 1166;
(b) W. Imhof, E. Anders, Chem. Eur. J. 10 (2004) 5717.
[5] J. Fleischhauer, R. Beckert, J. Weston, M. Schmidt, H.J. Flammersheim, H. Görls, Synthesis (2006) 514.
[6] (a) R. Siebenlist, H.-W. Frühauf, H. Kooijman, N. Veldman, A.L. Spek, K. Goubitz, J. Fraanje, Inorg. Chim. Acta 327 (2002) 66;
(b) M. DelaVarga, R. Costa, R. Reina, A. Núñez, M.Á. Maestro, J. Mahía, J. Organomet. Chem. 677 (2003) 101.
[7] (a) F.H. Allen, O. Kennard, D.G. Watson, L. Brammer, A.G. Orpen, R. Taylor, J. Chem. Soc., Perkin Trans. 2 (1987) S1;
(b) A.G. Orpen, L. Brammer, F.H. Allen, O. Kennard, D.G. Watson, R. Taylor, J. Chem. Soc., Dalton Trans. (1989) S1.
[8] M. Hesse, H. Meier, B. Zeh, Spektroskopische Methoden in der organischen Chemie, fourth ed., Georg Thieme Verlag Stuttgart, New York, 1991.
[9] COLLECT, Data Collection Software; Nonius B.V., Netherlands, 1998.
[10] Z. Otwinowski, W. Minor, Processing of X-ray diffraction data collected in oscillation mode, in: C.W. Carter, R.M. Sweet (Eds.), Methods in Enzymology, Macromolecular Crystallography Part A, vol. 276, Academic Press, 1997, pp. 307–326.
[11] G.M. Sheldrick, Acta Crystallogr. A 46 (1990) 467–473.
[12] G.M. Sheldrick, SHELXL-97 (Release 97-2), University of Göttingen, Germany, 1997.